

Submitted:
13.02.2019
Accepted:
10.04.2019
Published:
28.06.2019

Monitoring the response to neoadjuvant chemotherapy in patients with breast cancer using ultrasound scattering coefficient: A preliminary report

Katarzyna Dobruch-Sobczak^{1,2}, Hanna Piotrkowska-Wróblewska¹,
Ziemowit Klimoda¹, Wojciech Secomski¹, Piotr Karwat¹,
Ewa Markiewicz-Grodzicka³, Agnieszka Kolasińska-Ćwikła³,
Katarzyna Roszkowska-Purska⁴, Jerzy Litniewski¹

¹ *Ultrasound Department, Institute of Fundamental Technological Research, Polish Academy of Sciences, Warsaw, Poland*

² *Radiology Department, M. Skłodowska-Curie Memorial Cancer Center and Institute of Oncology, Warsaw, Poland*

³ *Chemiotherapy Department, M. Skłodowska-Curie Memorial Cancer Center and Institute of Oncology, Warsaw, Poland*

⁴ *Zakład Patomorfologii, M. Skłodowska-Curie Memorial Cancer Center and Institute of Oncology, Warsaw, Poland*

Correspondence: Katarzyna Dobruch-Sobczak, Radiology Department, M. Skłodowska-Curie Memorial Cancer Center and Institute of Oncology, ul. Wawelska 15, 03-024 Warsaw, Poland; e-mail: kdsobczak@gmail.com

DOI: 10.15557/JoU.2019.0013

Keywords

integrated backscatter coefficient (IBSCs), neoadjuvant chemotherapy (NAC), breast cancer, ultrasound

Abstract

Objective: Neoadjuvant chemotherapy was initially used in locally advanced breast cancer, and currently it is recommended for patients with Stage 3 and with early-stage disease with human epidermal growth factor receptors positive or triple-negative breast cancer. Ultrasound imaging in combination with a quantitative ultrasound method is a novel diagnostic approach. **Aim of study:** The aim of this study was to analyze the variability of the integrated backscatter coefficient, and to evaluate their use to predict the effectiveness of treatment and compare to ultrasound examination results. **Material and method:** Ten patients (mean age 52.9) with 13 breast tumors (mean dimension 41 mm) were selected for neoadjuvant chemotherapy. Ultrasound was performed before the treatment and one week after each course of neoadjuvant chemotherapy. The dimensions were assessed adopting the RECIST criteria. Tissue responses were classified as pathological response into the following categories: not responded to the treatment (G1, cell reduction by $\leq 9\%$) and responded to the treatment partially: G2, G3, G4, cell reduction by 10–29% (G2), 30–90% (G3), $>90\%$ (G4), respectively, and completely. **Results:** In B-mode examination partial response was observed in 9/13 cases (completely, G1, G3, G4), and stable disease was demonstrated in 3/13 cases (completely, G1, G4). Complete response was found in 1/13 cases. As for backscatter coefficient, 10/13 tumors (completely, and G2, G3, and G4) were characterized by an increased mean value of 153%. Three tumors 3/13 (G1) displayed a decreased mean value of 31%. **Conclusion:** The variability of backscatter coefficient, could be associated with alterations in the structure of the tumor tissue during neoadjuvant chemotherapy. There were unequivocal differences between responded and non-responded patients. The backscatter coefficient analysis correlated better with the results of histopathological verification than with the B-mode RECIST criteria.

Introduction

Neoadjuvant chemotherapy (NAC) was initially used in locally advanced breast cancer (LABC) and the inflammatory form of cancer to downstage locally inoperable disease. Currently, it is recommended for patients with Stage 3 and with early-stage disease with HER-2 (human epidermal growth factor receptors positive or triple-negative (TNBC) breast cancer^(1,2). NAC reduces the tumor mass by inducing intracellular damage, which causes cell death and degeneration. Response to treatment increases chances for surgery, makes breast-conserving surgery more feasible and might lead to eradication of micrometastatic disease and reduction of the risk of dissemination^(3,4). This treatment gives us the opportunity to observe the tumor shrink, both palpably and on imaging, enabling an assessment of clinical response. It also provides additional information about chemosensitivity of cancer tissue to different NAC programs, allowing to modify the subsequent treatment. However, the response to NAC is heterogenous, and objective assessment is necessary to distinguish between responders and non-responders and, if necessary, to modify treatment. Response is defined and classified on the basis of changes in cancer cellularity and is divided into two categories: pathological partial response (pPR) subdivided into G1 (<9% reduction), G2 (10–29%), G3 (30–90%) and G4 (>90%), and pathological complete response (pCR)⁽⁵⁾. The rate of responding and non-responding patients varies: pCR is seen (depending on the results presented in the literature) in 10–31% of patients, while pPR is seen in 69% to 100% of patients^(6–8). (In our study G1 was adopted as non-responding patients).

Currently, in the monitoring of patients treated with NAC, clinical breast examination (CBE), mammography (MMG), traditional B-mode ultrasound imaging (US), magnetic resonance imaging with a contrast agent (CA-MRI), or diffusion-weighted magnetic resonance imaging (DW-MRI) can be used⁽⁹⁾. CBE has been shown to be a subjective technique with limited efficacy, especially in tumors smaller than 2 cm: about 60% of residual breast cancers are undetectable by CBE⁽¹⁰⁾.

Ultrasound is considered a more accurate method in assessing tumor size and monitoring residual breast tumors compared to CBE or MMG⁽¹¹⁾. The literature analyzing the usefulness of an ultrasound examination together with MMG describes an increase in the probability of pCR prediction by up to 80%⁽¹²⁾. A promising method for observing regression of the disease is contrast-enhanced ultrasound, but this test is not commonly used and not recommended by EFSUMB⁽¹³⁾.

Sonoelastography is another ultrasound technique used to monitor effectiveness of NAC. The published results suggest that a reduction in tumor stiffness observed by shear wave elastography (SWE) and strain elastography allows, with similar performance, to predict the response of the disease to NAC^(14–18). Evans *et al.*⁽¹⁴⁾ have demonstrated, using SWE, that a decrease in breast cancer stiffness evaluated after the 3rd course of NAC was a predictor of pCR with sensitivity of

59% and specificity of 85%. Jing *et al.* have demonstrated that decreasing stiffness in SWE (relative changes) could effectively predict the response to NAC after 2 cycles⁽¹⁷⁾.

Among the available radiological methods, the monitoring of tumor response during NAC using magnetic resonance imaging (MRI) is more accurate in comparison to CBE, US, or MMG. However, the access to MRI may be limited, and underestimation of residual disease may affect up to 20% of patients^(19,20). The limitations of radiological methods may be due to the fact that the tumor size and architecture changes are delayed with respect to cell death which begins several hours or days after the start of the treatment⁽²¹⁾. It has been shown that under the influence of NAC, the tumor microstructure, including cell number, changes before its macroscopic dimensions are affected^(21,22). In patients with pCR, areas of early tumor invasion display fibrosis and edema of the stroma with increased vascularization and infiltration of inflammatory cells⁽²³⁾. For non-responding patients (pPR G1), tumor cells remain almost unchanged. However, in patients with pPR: G2, G3, G4, there is a change in the percentage of enlarged, multinucleated and neoplastic cells^(23,24).

New, easy diagnostic tools are sought that will differentiate patients who respond to treatment from non-responders to NAC with high accuracy and at an early stage of treatment. In the literature, there are publications on the usefulness of quantitative ultrasound (QUS) techniques for monitoring reactions to NAC^(24–27). In the case of a classic B-mode examination, the image is created on the basis of an envelope of radio-frequency (RF) signals, which is subjected to intensive downstream processing. Filtration, log-compression, interpolation, and image enhancing algorithms are used to reduce noise and reveal details of the tissues on the ultrasound scanner screen. These procedures, however, reduce the amount of information about the examined tissues, which can be obtained from the analysis of original RF signals. QUS techniques use raw RF echo signals back-scattered on elements included in examined tissues, such as neoplastic cell clusters or elements of fibrous stromal tissue in the mammary gland.

The theory of acoustic scattering in relation to tissue biology and the assessment of the usefulness of various ultrasound techniques for the study of cellular density has been analyzed by, among others, Oelze *et al.*⁽²⁸⁾. Since then, many QUS methods have been developed based on the analysis of the scattered echo with the aim to characterize the microstructure and elastic properties of tissues. Ultrasonic parameters determined from the scattered echo that can characterize the microstructure of tissues include statistical parameters of the echo envelope^(29,30), texture parameters⁽³¹⁾, and scattering parameters. The latter can effectively predict the response of tumor tissue to the used treatment^(26,31).

The aim of our study was to evaluate patient responses to NAC using different ultrasound techniques, namely the assessment of tumor size in B-mode imaging, stiffness assessment in elastography examination and using

quantitative ultrasound parameter. As a quantitative measure, we applied the integrated backscatter coefficient (IBSC), whose value depends on the quantity, shape, organization and size of the scattering elements.

Material and methods

Patients

The study protocol was approved by the institutional review board of the Maria Skłodowska-Curie Memorial Cancer Centre and Institute of Oncology in Warsaw, Poland. All patients gave their written consent to participate in the study. From April 2016 to November 2017, 10 patients aged 32 to 75 (mean age 52.9) with a total of 13 tumors (one bifocal lesion, one trifocal lesion) were deemed eligible for NAC at the Oncology Clinic. AT (doxorubicin, docetaxel), AC (doxorubicin, cyclophosphamide) and paclitaxel were used in the treatment, according to international guidelines. All patients underwent simple mastectomy with lymphadenectomy.

Histology

All patients underwent core needle biopsies (CNB) after administration of 2% lidocaine, using a biopsy gun needle (14G diameter – Pro-Mag). Three to five cores were taken from each lesion. After surgery (simple mastectomy), surgical specimens were immediately fixed in 10% buffered formalin. Representative sections from these samples were processed and routinely stained for histopathological (microscopic) examinations (HE). All tumor samples were

evaluated by the same pathologist. Based on the pathological assessment of breast tissue the following information was obtained: grade of malignancy, cancer subtype, reduction in cancer cells, and residual tumor size (Tab. 1, Tab. 2, Tab. 3). In order to categorize the tumor's pathological response to NAC, changes in cellularity of tumors were quantified using the samples obtained from the CNB before treatment and the material obtained after the treatment and surgery, using the Miller-Payne scale⁽⁵⁾. In histopathological examination after NAC, tumors were classified into two categories: pathological partial response (pPR) and pathological complete response (pCR). pPR was subdivided into G1, G2, G3, or G4, according to the extent of the changes observed. The results of the ultrasonic analysis were referred to the pathological verification.

Registration of ultrasonic data

A total of 67 B-mode ultrasound examinations with breast sonoelastography and lymph node assessment were performed in the Department of Ultrasound, Institute of Fundamental Technological Research, Polish Academy of Science in Warsaw.

B-mode images and the corresponding raw RF echoes were recorded using an ultrasound scanner (Ultrasonix SonixTouch, Ultrasonix Medical Corporation, Richmond, BC, Canada) and a linear array transducer L14-5/38, with the transmitted frequency set at 10 MHz, which, as measured by a hydrophone, corresponded to pulses center frequency of approximately 7.5 MHz. The tumor area region of interest (ROI) was determined on the B-mode image by an experienced radiologist.

Tab. 1. Breast tumor sizes before and after treatment as revealed in B-mode imaging, sonoelastography and final histopathological examinations

Patient n	Tumor size before treatment (W × D × L) in mm	Tumor size after treatment (W × D × L) in mm (Reduction in length compared to the initial result in %) RECIST 1.1 results	Tsukuba scale before/after treatment	Tumor size in final histopathological examination (mm)
1	8 × 10 × 9	4 × 3 × 3 (67%) PR	2/4	4 × 5 × 5
2a	19 × 27 × 17	12 × 7 × 8 (53%) PR	4/2	25 × 22 × 20
2b	35 × 41 × 36	9 × 9 × 6 (84%) PR	4/2	35 × 45 × 25
3	25 × 27 × 26	6 × 6 × 7 (73%) PR	4/3	40 × 30 × 20
4	20 × 23 × 25	10 × 8 × 12 (52%) PR	2/2	25 × 17 × 25
5	9 × 20 × 13	6 × 13 × 4 (69%) PR	5/5	22 × 17 × 18
6	22 × 13 × 21	18 × 20 × 11 (48%) PR	4/4	35 × 17 × 12
7	25 × 17 × 15	14 × 6 × 11 (27%) SD	4/2	13 × 12 × 11
8	30 × 21 × 41	20 × 16 × 34 (17%) SD	4/4	30 × 30 × 41
9	10 × 24 × 16	10 × 14 × 9 (44%) PR	2/2	0
10a	17 × 10 × 21	5 × 5 × 8 (62%) PR	3/4	9 × 7 × 11
10b	3 × 10 × 8	2 × 8 × 6 (25%) SD	3/3	0
10c	5 × 5 × 4	** CR	2/2*	0

W – width, D – depth, L – length, % reduction in the largest dimension of the radial plane lesion
* Assessment of elastography after 2nd course of NAC; ** Lesion invisible from the week after the end of the 3rd course of NAC

Tab. 2. Results of histopathological verification from core-needle biopsy and applied treatment

Patient n	Pathology	Grade	ER %	PGR %	HER 2+	Ki-67 %	IHCH type	NAC type
1	NST	2	100	80	3	70	Luminalny B HER 2+	AT
2a, b	NST	2	100	50	0	30	Luminalny B HER2–	AT and Taxotere
3	NST	2	0	0	3	30	HER 2+	AT
4	NST	2	90	85	–	2	Luminalny A	AC and paklitaksel
5	NST	1	100	80	–	2	Luminalny A	Tamoksyfen
6	NST	2	80	40	1	2	Luminalny A	AC and paklitaksel
7	NST	2	70	75	0	10	Luminalny A	AC
8	NST	2	100	40	1	15	Luminalny A	AC
9	NST + CDIS	2	90	40	1	30	Luminalny B HER 2–	AC and paklitaksel
10a, b, c	NST	3	100	60	–	60	Luminalny B HER 2–	AC and paklitaksel

NST – nonspecific type; ER – estrogen receptor; PGR – progesterone receptor; HER – human epithelial growth factor; AT – doxorubicin, docetaxel; AC – doxorubicin, cyclophosphamide; IHCH – immunohistochemical examination

Each patient underwent at least five ultrasound examinations: baseline recordings were made before the start of the treatment, with subsequent scans conducted a week after each round of chemotherapy.

During each examination, the data from the focal lesion were recorded from four cross-sections (radial, radial+45°, anti-radial, anti-radial+45°). The period of participating patient monitoring was 5–6 months.

The assessment of tumors was based on the guidelines of the American College of Radiology (BI-RADS lexicon) and the standards of the Polish Ultrasound Society^(32,33). The RECIST 1.1 classification was adapted to monitor the longest diameter of tumors⁽³⁴⁾ even though RECIST guidelines state that US is unsuitable for monitoring the tumor size because it is operator-dependent (partial response (PR), stable disease (SD), complete response (CR), and progressive disease (PD)). Similar RECIST criteria to predict response during NAC were used by Marinovich ML *et al.*⁽³⁵⁾.

Tsukuba scale was used in the sonoelastographic assessment of tumors⁽³⁶⁾. It is a 5-point scale of classification, from Tsukuba 1, denoting strain present in the whole

Tab. 3. Microscopic assessment of tumor cell damage and tumor mass after chemotherapy

Patient n	Reduction in cancer cells (%)	Classification of histopathology
1	100%	pCR
2a, b	60%	G3
3	85%	G3
4	30%	G3
5	0%	G1
6	0%	G1
7	91%	G4
8	0%	G1
9	100%	pCR
10a	95%	G4
10b	100%	pCR
10c	100%	pCR

lesion, to Tsukuba 5, denoting no strain detected in the lesion and surrounding tissue (see Fig. 1B, Fig. 2B, Fig. 3B and Fig. 4B).

In order to collect data for quantitative analysis for each B-mode scan, 510 RF signal lines were recorded at the sampling frequency of 40 MHz. The transducer's focus was always sited in the middle of the lesion. The analysis of the collected data for IBSC determination was performed offline using proprietary programs implemented in the Matlab environment (Mathworks, Natick, MA, USA).

Quantitative ultrasound parameters

Integrated backscatter coefficient (IBSC)

The analysis of RF signals to determine IBSC was carried out using the method proposed by Yao *et al.*⁽³⁷⁾. The ROI (tumor area) was analyzed using a sliding window method. The window was moved horizontally with a step corresponding to a distance between successive RF lines (0.08 mm) and vertically with a step of one sample of the analyzed signal (0.02 mm). Parametric maps showing changes occurring due to NAC were built on the basis of IBSC values found in subsequent windows in the tumor area. Higher values of IBSC are represented as red and lower values as blue. In order to determine a single IBSC value characterizing the entire lesion, IBSC values obtained for all windows in a given section of the tumor were averaged, and the mean of four sections was then used.

Results

B-mode ultrasound imaging

In this study the 10 patients underwent simple mastectomy with lymphadenectomy after chemotherapy. The largest dimensions in the radial plane (according to RECIST 1.1) were in 4–41 mm range before treatment

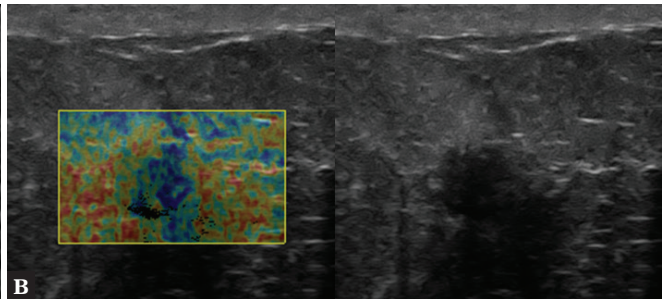
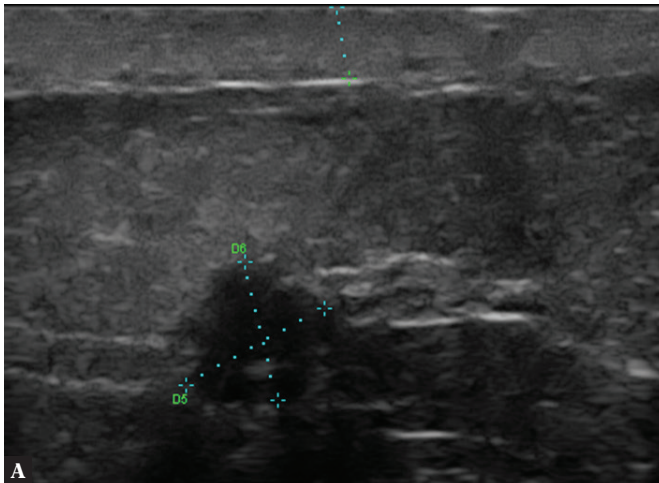


Fig. 1. A. B-mode images of Patient 1 present a hypoechoic, rounded, solid lesion, with lobular margins, without visible calcification, confirmed in histopathological verification as IC NST. **B.** Strain elastogram shows a Tsukuba 2 lesion. Stiff tissues are coded in red color, deformable in blue, and intermediate in green

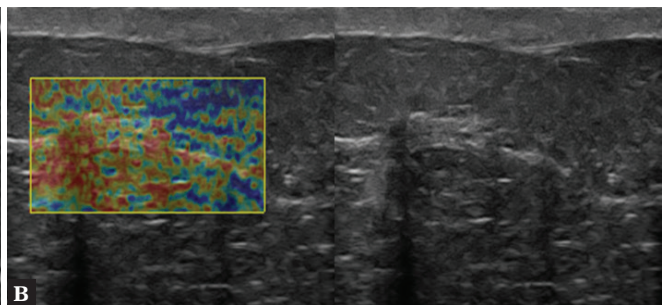
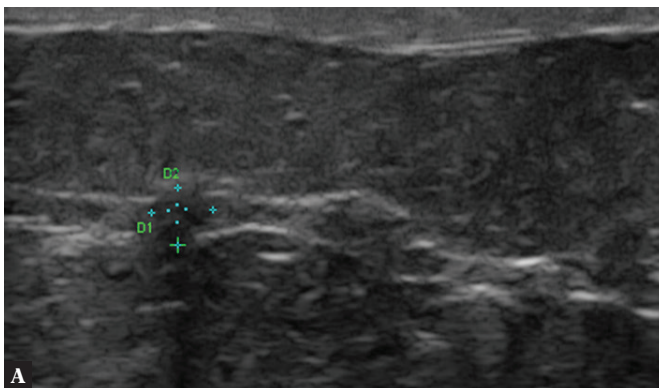


Fig. 2. A. B-mode image after NAC in Patient 1 presents an isoechoic lesion with irregular edges. **B.** Strain elastogram shows a Tsukuba 4 lesion

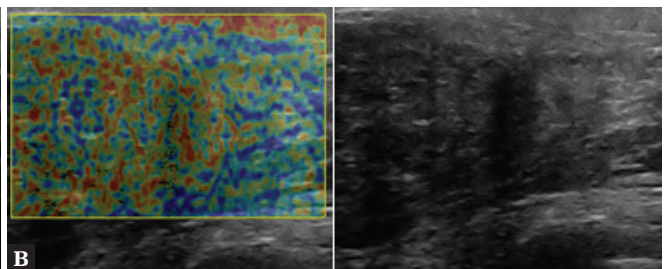
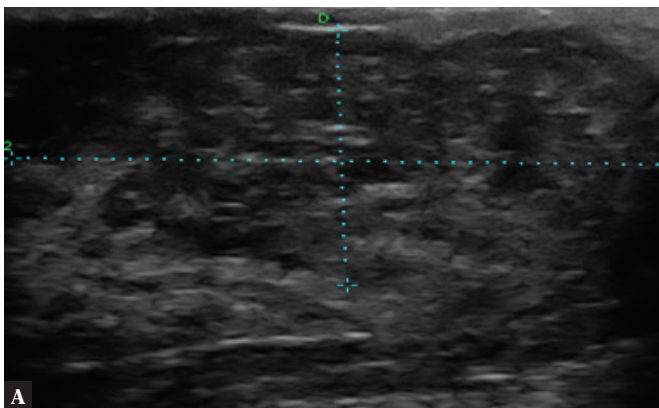


Fig. 3. A. B-mode image of Patient 8 before NAC presents an irregular, heterogeneous, hypoechoic solid lesion, with indistinct margins. **B.** Elastography predominates no strain in the tumor (Tsukuba 4)

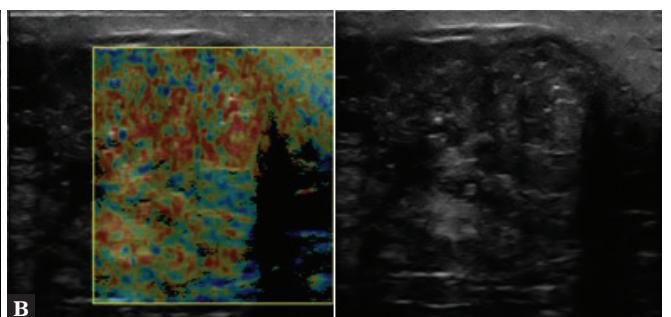
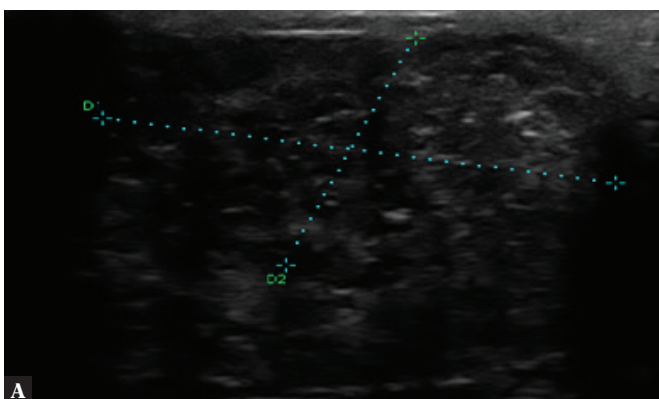


Fig. 4. A. B-mode image of Patient 8 after NAC presents a heterogeneous, hypoechoic and solid lesion. **B.** Elastography shows a Tsukuba 4 lesion

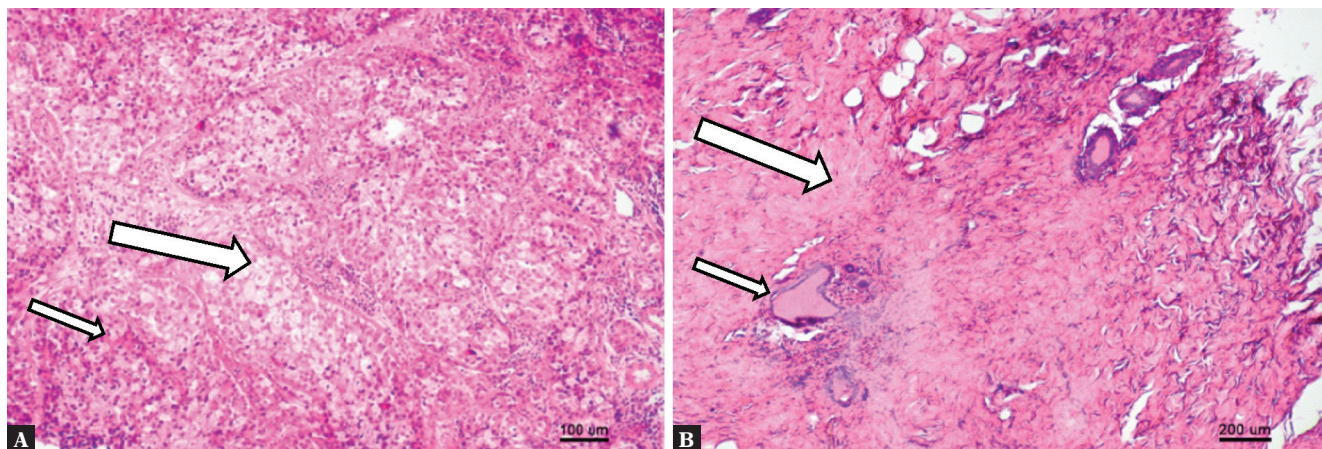


Fig. 5. **A.** Microscopic image of Patient 1 core-needle biopsy before treatment. The thick arrow indicates neoplastic cells and accompanying lymphocyte infiltration (thin arrow). **B.** Microscopic image of Patient 1 after treatment presents visible milk ducts (thin arrow) and stromal tissue (thick arrow), no visible neoplastic cells

and in 3–34 mm range after treatment. The dimensions of neoplastic tumors decreased. Partial response (PR – $\geq 30\%$ reduction of the longest diameter of the primary tumor) was observed in 9 of 13 cases which were histopathologically classified as pCR, G1, G3, or G4. In 3 of 13 lesions, stable disease (SD) was demonstrated (HE indicated pCR, G4, G1). In one case, which was classified in HE as pCR, the ultrasound examination also showed complete response (CR).

The results of ultrasound examinations (B-mode tumor size and elastography, before and after NAC) and the tumor size after pathological examinations are presented in Tab. 1. Elastography assessed after treatment, designated 5 of 13 tumors as non-deformable. These consisted of 3 tumors that did not respond to treatment (pPR G1) and were characterized by high stiffness (T4 and T5), one pCR tumor, and 1 pPR G4 tumor. In 4 of 13 cases, there was a decrease in stiffness (in HE, pPR lesions: G3 and G4). In 2 tumors, an increase in stiffness was observed; these were a pCR tumor and a pPR G4 tumor. In 7 of 13 tumors, stiffness did not change (in HE, pPR lesions: G1, G3 and pCR).

Results of histopathological verification

Histopathological examination after NAC and surgery revealed 4 pCR tumors. The remaining lesions were pPR (including 3 G1 cases). Lesions were verified as G2 and G3 invasive carcinoma non-specified type (IC NST) (Tab. 2). Table 3 presents the percentage reduction of cancer cells and histopathological verification performed after NAC.

The images from microscopic verification and the corresponding images from the B-mode examination before and after treatment for two patients with extremely different responses to the treatment (cases 1 and 8) are presented in Fig. 1, Fig. 2, Fig. 3, Fig. 4, Fig. 5, Fig. 6 below. Patient 1 responded to NAC (pCR), while patient 8 did not respond to the treatment (G1).

Quantitative backscatter ultrasound results

Ten tumors which were classified by histopathological examination after NAC as pathological complete response (pCR) and pathological partial response (G2, G3, and G4) were characterized by an increase in the IBSC value, being in the

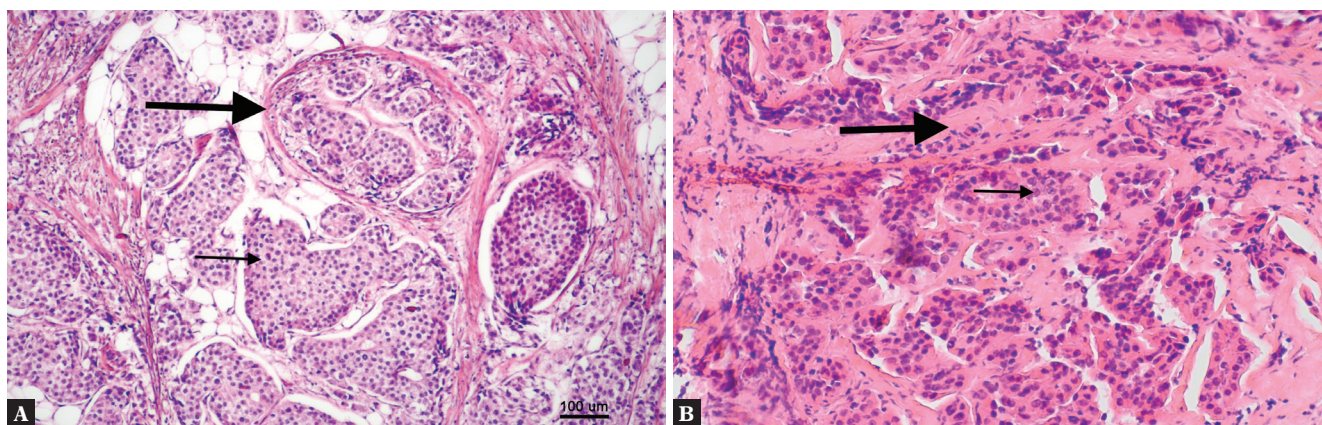


Fig. 6. **A.** Microscopic image of Patient 8 presents clusters of tumor cells from core-needle biopsy (thin arrow) and a band of fibrous tissue (thick arrow). **B.** Tumor cells after treatment in Patient 8: neoplastic cells (thin arrow) and stroma (thick arrow) with features of minor damage

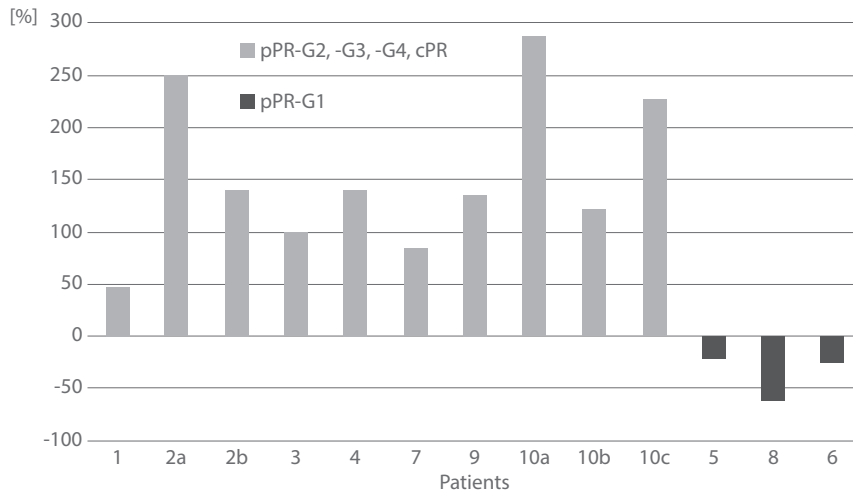


Fig. 7. Percentage change of the IBSC value after NAC

range from 48% to 287% (mean 153%). Three tumors that were designated as pPR G1 (<9% reduction in cancer cellularity) displayed a decrease in IBSC in the range from -20% to -60% (mean -31%). Figure 7 shows the percentage change of IBSC value after NAC. The IBSC value for each lesion prior to the start of the treatment was used as a reference value.

Discussion

The analysis of B-mode ultrasound images of 13 breast tumors using an adapted RECIST 1.1 methodology indicated partial response in 9, complete response in 1, and stable disease in 3 tumors. This assessment, however, did not correlate with the dimensions and cellularity of tumors obtained in the final histopathological verification. In tumors with partial response and stable disease, pathological response G1, but also G3, G4, and pCR were observed. It is worth noting that the dimensions of tumors obtained in the final histopathological verification were much larger than the dimensions determined on the basis of B-mode imaging.

In our study, there was no correlation of changes in the stiffness of tumors (sonoelastography) with other methods used to demonstrate a response to treatment (QUS or histopathology). The studies published so far have shown that both sonoelastography techniques (relative strains and SWE) are useful in predicting responses to NAC. Ma Y *et al.* showed in a group of 71 patients that a decrease in mean E and SR (Strain Ratio) after courses of chemotherapy predicted the response to treatment with high accuracy (AUC = 0.93 and 0.90, respectively)⁽¹⁶⁾. They also pointed out that lower initial tumor stiffness correlated with a favorable response after NAC (pCR). Similar results were obtained by Hayashi⁽¹⁸⁾, where the authors concluded that the group with low scores in the Tsukuba scale (1–3) had significantly higher clinical complete response and pCR rates than the high EG group (pCR, low EG group 50 % vs high EG group 14 %, $P = 0.003$, respectively).

A detailed analysis of pCR tumors using sonoelastography in our study demonstrated no changes or reduced stiffness. In the histopathological evaluation of these pCR lesions, all patients displayed a significant decrease in tumor cellularity compared to CNB (core-needle biopsy). The samples appeared to contain fibrosis and stromal elastosis, which could increase tumor stiffness, but this was demonstrated only in one patient in our study. Different results were obtained for the assessment of tumors using QUS, including tumors with pCR. There were large differences in IBSC values between the group of tumors which responded to the treatment (pCR, pPR G2, G3, and G4) and the group that did not respond to the treatment (pPR G1). In the first group, there was an increase in the IBSC value, while in the second group, there was a slight decrease.

Similar results were published by Sannachi *et al.*: 30 patients with LABC showed no changes in IBSC values in a group of non-responders. The authors, however, defined non-response as no significant differences in the microscopic assessment of cellularity of lesions and less than 50% reduction in the tumor size⁽²⁶⁾.

Bearing in mind our results and reports from the literature, we question what constitutes the main source of scattering in breast tumors being examined. Czarnota *et al.* hypothesized that it is possible to observe cell nucleus defragmentation during apoptosis using high ultrasonic frequencies (>20 MHz)⁽³⁸⁾. The influence of cell properties on ultrasound scattering has been confirmed by, among others, Czarnota and Kolios who demonstrated an *in vitro* correlation of the size of an apoptotic cell nucleus with the scattering intensity indicated by IBSC^(39,40).

Nevertheless, the hypothesis of an observed increase in ultrasound scattering as a result of defragmentation of cell nuclei cannot be directly extrapolated to our *in vivo* studies of breast cancer. The length of ultrasonic waves at 7.5 MHz used in our work is relatively large, and thus the

wave does not interact directly with individual cells but with larger tissue structures, such as cell clusters or stromal fibroid tissue. The relationship between the change of IBSC and the changes occurring in tissue structure should therefore be considered at the level of reconstruction of whole cell clusters or remodeling of the stroma during chemotherapy.

The interpretation of the alteration in ultrasound backscattered parameters is problematic. The spatial distribution of tissue types and their effect on ultrasonic scattering are not wholly understood. In addition, the results of histopathological examination only provide information about the condition of a part of the tumor tissue before NAC (taken by biopsy) and after the entire treatment cycle, and may not be reflective of the changes taking place after each NAC course.

Conclusions

Early prediction of response to NAC in patients with breast cancer is crucial for planning further therapy and surgery. This is the first report comparing ultrasound-based tumor size assessment, sonoelastography and quantitative ultrasonography with histopathological findings in patients undergoing neoadjuvant chemotherapy. Preliminary results in a group of 10 female patients with 13 breast cancer tumors confirmed the relationship between the results of post-operative histopathological verification and changes in the IBSC value. In the study group, there were unequivocal differences in IBSC values between patients with pCR lesions, pPR tumors (G2, G3, G4) and patients without changes in cellularity after treatment (pPR G1). The results were not as

unambiguous in the assessment of the tumor size in the B-mode study and deformability changes in sonoelastography. The QUS technique, and in particular the IBSC parameter, may supplement the methods of assessing the effectiveness of treatment with NAC. In order to determine whether IBSC extends clinical benefit in the NAC assessment, further observations using a larger cohort of patients are necessary.

Acknowledgment

This study was supported by the National Science Centre, Poland, grant 2016/23/B/ST8/03391

Conflict of interest

All authors declare that they have no conflicts of interest.

Ethical approval

All the procedures performed in the study that involved human participants were in accordance with the ethical standards of the Maria Skłodowska Curie Memorial Cancer Centre and the Institute of Oncology research committee and followed guidelines set by the 1964 Helsinki Declaration and its later amendments or comparable ethical standards.

Informed consent

Informed consent was obtained from all individual participants included in the study.

References

1. Morigi C: Highlights from the 15th St Gallen International Breast Cancer Conference 15–18 March, 2017, Vienna: tailored treatments for patients with early breast cancer. *Ecancermedalscience* 2017; 11: 732.
2. Giordano SH: Update on locally advanced breast cancer. *Oncologist* 2003; 8: 521–530.
3. Berruti A, Amoroso V, Gallo F, Bertaglia V, Simoncini E, Pedersini R *et al.*: Pathologic complete response as a potential surrogate for the clinical outcome in patients with breast cancer after neoadjuvant therapy: A meta-regression of 29 randomized prospective studies. *J Clin Oncol* 2014; 34: 3883–3891.
4. Early Breast Cancer Trialists' Collaborative Group (EBCTCG): Long-term outcomes for neoadjuvant versus adjuvant chemotherapy in early breast cancer: meta-analysis of individual patient data from ten randomised trials. *Lancet Oncol* 2018; 19: 27–39.
5. Ogston KN, Miller ID, Payne S, Hutcheon AW, Sarkar TK, Smith I *et al.*: A new histological grading system to assess response of breast cancers to primary chemotherapy: prognostic significance and survival. *Breast* 2003; 12: 320–327.
6. Maur M, Guarneri V, Frassoldati A, Conte PF: Primary systemic therapy in operable breast cancer: clinical data and biological fall-out. *Ann Oncol* 2006; 17 (Suppl. 5): v158–v164.
7. Sachelarie I, Grossbard ML, Chadha M, Feldman S, Ghesani M, Blum RH: Primary systemic therapy of breast cancer. *Oncologist* 2006; 11: 574–589.
8. von Minckwitz G, Untch M, Blohmer JU, Costa SD, Eidtmann H, Fasching PA *et al.*: Definition and impact of pathologic complete response on prognosis after neoadjuvant chemotherapy in various intrinsic breast cancer subtypes. *J Clin Oncol* 2012; 30: 1796–1804.
9. Dialani V, Chadashvili T, Slanetz PJ: Role of imaging in neoadjuvant therapy for breast cancer. *Ann Surg Oncol* 2015; 22: 1416–1424.
10. Cocconi G, Di Blasio B, Alberti G, Bisagni G, Botti E, Peracchia G: Problems in evaluating response of primary breast cancer to systemic therapy. *Breast Cancer Res Treat* 1984; 4: 309–313.
11. Bosch AM, Kessels AG, Beets GL, Rupa JD, Koster D, van Engelshoven JM *et al.*: Preoperative estimation of the pathological breast tumor size by physical examination, mammography and ultrasound: a prospective study on 105 invasive tumours. *Eur J Radiol* 2003; 48: 285–292.
12. Keune JD, Jeffe DB, Schootman M, Hoffman A, Gillanders WE, Aft RL: Accuracy of ultrasonography and mammography in predicting pathologic response after neoadjuvant chemotherapy for breast cancer. *Am J Surg* 199; 477–484.
13. Corcioni B, Santilli L, Quercia S, Zamagni C, Santini D, Taffurelli M, Mignani S: Contrast-enhanced US and MRI for assessing the response of breast cancer to neoadjuvant chemotherapy. *J Ultrasound* 2008; 11: 143–150.
14. Evans A, Whelehan P, Thompson A, Purdie C, Jordan L, Macaskill J *et al.*: Prediction of pathological complete response to neoadjuvant chemotherapy for primary breast cancer comparing interim ultrasound, shear-wave elastography predict and MRI. *Ultraschall Med* 2017; 39: 422–431.
15. Evans A, Armstrong S, Whelehan P, Thomson K, Rauchhaus P, Purdie C *et al.*: Can shear-wave elastography predict response to neoadjuvant

- chemotherapy in women with invasive breast cancer? *Br J Cancer* 2013; 109: 2798–2802.
16. Ma Y, Zhang S, Li J, Jianyi Li, Kang Y, Ren W: Comparison of strain and shear-wave ultrasonic elastography in predicting the pathological response to neoadjuvant chemotherapy in breast cancers. *Eur Radiol* 2016; 27: 2282–2291.
 17. Jing H, Cheng W, Li ZY, Ying L, Wang QCh, Wu T, Tian JW: Early evaluation of relative changes in tumor stiffness by shear wave elastography predicts the response to neoadjuvant chemotherapy in patients with breast cancer. *J Ultrasound Med* 2016; 35: 1619–1627.
 18. Hayashi M, Yamamoto Y, Ibusuki M, Fujiwara S, Yamamoto S, Tomita S *et al.*: Evaluation of tumor stiffness by elastography is predictive for pathologic complete response to neoadjuvant chemotherapy in patients with breast cancer. *Ann Surg Oncol* 2012; 19: 3042–3049.
 19. Lobbes M, Prevos R, Smidt M: Response monitoring of breast cancer patients receiving neoadjuvant chemotherapy using breast MRI – a review of current knowledge. *J Cancer Ther Res* 2012; 1: 34–43.
 20. Dialani V, Chadashvili T, Slanetz PJ: Role of imaging in neoadjuvant therapy for breast cancer. *Ann Surg Oncol* 2015; 22: 1416–1424.
 21. Sadeghi-Naini A, Papanicolaou N, Falou O, Zubovits J, Dent R, Verma S *et al.*: Quantitative ultrasound evaluation of tumor cell death response in locally advanced breast cancer patients receiving chemotherapy. *Clin Cancer Res* 2013; 19: 2163–2174.
 22. Brindle K: New approaches for imaging tumour responses to treatment. *Nat Rev Cancer* 2008; 8: 94–107.
 23. Briffod M, Spyrtos F, Tubiana-Hulin M, Pallud C, Mayras C, Filleul A, Rouëssé J: Sequential cytopunctures during preoperative chemotherapy for primary breast carcinoma. Cytomorphologic changes, initial tumor ploidy, and tumor regression. *Cancer* 1989; 63: 631–637.
 24. Kennedy S, Merino MJ, Swain SM, Lippman ME: The effects of hormonal and chemotherapy on tumoral and nonneoplastic breast tissue. *Hum Pathol* 1990; 21: 192–198.
 25. Sadeghi-Naini A, Sannachi L, Tadayyon H, Tran W, Slodkowska E, Trudeau M *et al.*: Chemotherapy-response monitoring of breast cancer patients using quantitative ultrasound-based intra-tumour heterogeneities. *Sci Rep* 2017; 7: 10352.
 26. Sannachi L, Tadayyon H, Sadeghi-Naini A, Tran W, Gandhi S, Wright F *et al.*: Non-invasive evaluation of breast cancer response to chemotherapy using quantitative ultrasonic backscatter parameters. *Med Image Anal* 2015; 20: 224–236.
 27. Tadayyon H, Sannachi L, Gangeh M, Sadeghi-Naini A, Tran W, Trudeau ME *et al.*: Quantitative ultrasound assessment of breast tumor response to chemotherapy using a multi-parameter approach. *Oncotarget* 2016; 7: 45094–45111.
 28. Oelze ML, Zachary JF, O'Brien WD Jr: Characterization of tissue microstructure using ultrasonic backscatter: theory and technique for op